ISSN (Print) 1226-1750
ISSN (Online) 2233-6656
Journal of Magnetics 28(1), 6-15 (2023) https://doi.org/10.4283/JMAG.2023.28.1.006

Design and Performance Study of Hybrid Channel-valved Magnetorheological Dampers

Yan Li[1], Xiaolong Yang[1]*, Jiehong Zhu[1], and Youming Zhou[2]

[1]*School of Mechanical and Automotive Engineering, Guangxi University of Science and Technology, Liuzhou 545006, China*
[2]*Dongfeng Liuzhou Motor CO., LTD, Liuzhou 545006, China*

(Received 20 October 2022, Received in final form 19 January 2023, Accepted 25 January 2023)

In order to solve the problem of low damping force caused by low utilization of magnetic field in traditional magnetorheological dampers, a hybrid channel valve type magnetorheological damper with circular channel and disk channel are proposed. The main content of this paper is to design the basic structure of mixed channel valve magnetorheological damper. The mathematical model of damping force based on Bingham plastic model was established from the design of magnetic circuits. The two-dimensional simulation model of MR Damper was established by using EMAG module in ANSYS finite element analysis software, and the magnetic circuit of mixed channel valve MR Damper was simulated and analyzed. The results show that the output damping force of the hybrid channel valve-type magnetorheological damper is 18 KN and the adjustable coefficient is 14.52 with the current *I* of 3*A*, the number of coil turns of 560, the axial damping gap of 1 mm and the radial damping gap of 1.5 mm.

Keywords : Magnetorheological dampers, Hybrid channel, Valved, Damping force, Performance analysis

1. Introduction

Since heavy trucks are in a harsh working environment for a long time, the vibration problem of heavy truck vehicles should draw our attention more. According to the research scholars, the impact of vibration on drivers and passengers is not only physiological, but also psychological. The physiological impact can bring various problems throughout the body, such as herniated discs, back pain and so on. The psychological impact is more serious, easy to occur irritability, psychological imbalance problems may lead to traffic accidents. In order to improve the vibration environment for heavy truck drivers and passengers brought harm, research scholars proposed the cab suspension system. Magnetorheological dampers as an important part of the cab suspension system are worthy of further study by research scholars.

Magnetorheological fluid is a new smart material that can rapidly achieve reversible and controlled conversion between solid and liquid states under the action of a magnetic field, which was first discovered in 1984 by Robinow [1], an American scholar. It is mainly formed by the homogeneous dispersion of magnetic particles in the base-loaded liquid. In order to prevent the precipitation of magnetic particles due to prohibition for a long time [2], increasing additives inhibits such problems. inhibit such problems. Magnetorheological dampers with magnetorheological fluid as the working medium is a kind of highly efficient semi-active controllable variable damping devices with many advantages such as simple structure, high damping force, fast response, continuously adjustable damping force and low energy consumption, which are widely used. They are mainly used in seat suspension, bridge damping, house damping, aircraft landing gear damping, ship damping [3-7] and other fields. In the actual application condition, magnetorheological dampers will be limited by their own volume due to different application scenarios, and it is necessary to study how to reasonably improve the damping performance of magnetorheological dampers at a certain volume.

Since the key factor affecting the damping force of the damper is the effective fluid flowing channel that can produce magnetorheological effect, how to reasonably and effectively improve the utilization of the fluid flowing channel is the current research interest of domestic and foreign scholars. Hu Guoliang *et al.* [8] designed a hybrid flow type magnetorheological damper, the liquid flow channel of which consists of four axial annular channels

*Corresponding author: Tel: +8618307721513
Fax: +8618307721513, e-mail: yangxiaolong@gxust.edu.cn

mixed with two radial disk channels in series, which effectively improves the damping performance of the damper by guiding the direction of the magnetic force lines. Jun Zhu *et al.* [9] proposed a magnetorheological damper with a radial channel along the annulus in order to improve the damping performance of the damper. In the article, the structure and magnetic circuit of the damper were designed. The dampers were analyzed and tested using MATLAB/Simulink and vibration experiments. The results show that the damping force is significantly increased and the adjustable range is widely compared with the common magnetorheological damper, which verifies the rationality of the damper design. Yi Han *et al*. [10] proposed a design method for a new parallel disc slotted magnetorheological damper, and this damper has the advantages of high efficiency, high sensitivity, and good heat dissipation. The results show that the tensile damping of this damper is greater compared with the compression damping force, and the maximum damping force can reach 15 *KN*. Guoliang Hu [11] *et al*. proposed a new magnetorheological damper with tandem flow channels and the structure showed that: the magneto-rheological damper has high vibration control capability and good mechanical properties. Also Senkal *et al.* [12], Kim *et al*. [13], Zemp *et al.* [14], Yazid *et al.* [15] have innovated the structure and all of them have achieved good conclusions.

A hybrid channel valved magnetorheological damper is proposed in the paper. The damper adopts a double-outlet rod with a valved mode of operation, and its fluid flow channel mainly consists of a 5-segment circular channel and a 4-segment disc channel. Through multiple simulations in ANSYS, the size and placement of the magnetically conductive parts and magnetic separation materials were fine-tuned. The magnetic lines of force can pass through the liquid flowing channel more perpendicularly, thus improving the utilization of the liquid flow channel. The preliminary structure is analyzed to calculate the saturation magneto-dynamic potential and establish the corresponding mathematical model of damping force and adjustable range. Finally, the variation of magnetic induction intensity at each fluid flow channel with different currents, different axial gaps and different radial gaps is obtained by ANSYS electromagnetic field simulation analysis. The output damping force and the adjustable range of damping force are analyzed numerically by MATLAB.

2. Structure and Working Principle

The hybrid channel valve magnetorheological damper is developed to reduce the irreversible damage caused by cab vibration to the driver, and its basic structure is a double outlet rod, compared to the shear working mode, the valve working mode can provide greater damping force, so the hybrid channel valve magnetorheological damper working mode is selected valve mode. The working principle of magnetorheological dampers is that a magnetic field is generated when the coil is energized. If the direction of the magnetic lines of force is perpendicular to the flow direction of the magnetorheological fluid in the fluid flowing channel, the magnetorheological fluid will occur a magnetorheological effect under the action of the magnetic field, thus producing a damping force, at which time the fluid flow channel is called an effective damping channel. Therefore, in order to improve the performance of magnetorheological dampers it is necessary to enhance the effective damping channel based on the growth of liquid flowing length. In this paper, a hybrid channel valve type magnetorheological damper is designed. As shown in Fig. 1, a two-dimensional plan view of a hybrid channel valved magnetorheological damper is shown, which mainly consists of a piston rod, a damper upper end cap, a damper cylinder wall, a valved piston head, and a damper lower end cap.

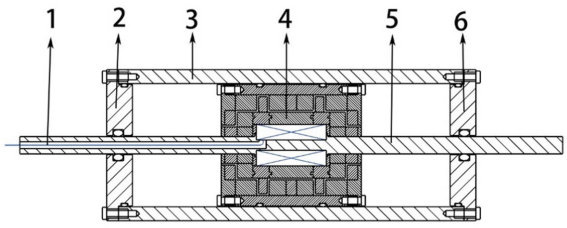

1: lead hole; 2: damper upper end cap; 3: damper cylinder wall; 4: Valved piston head; 5: piston rod; 6: damper lower end cap.

Fig. 1. Hybrid channel valved magnetorheological damper.

Figure 2 shows a two-dimensional schematic diagram of the valved piston head of the hybrid channel valved magnetorheological damper, as shown in the figure, the valved piston head of the hybrid channel valved magnetorheological damper mainly consists of the top covor of the piston, the magnetic conducting disc a, the magnetically insulated circular ring a, the magnetic conducting ring a, the magnetic conducting disc b, the magnetic conducting ring b, the magnetic isolation ring b, the magnetic conducting ring c, the outer wall of the piston head, the magnetic isolation ring c, the winding frame, the magnetic conducting ring d, the magnetic conducting ring e, and the lower end cap of the piston head. The magnetic isolation ring a and the magnetic conducting ring e near the piston rod, both of which are

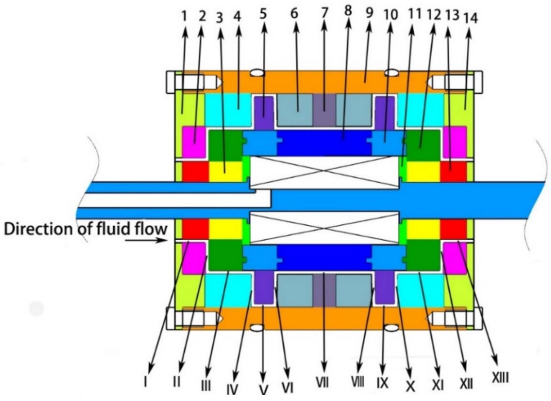

1: upper end caps of the piston; 2. magnetically conducting disc a; 3. magnetically isolated circle a; 4. magnetically conducting circle a; 5. magnetically conducting disc b; 6. magnetically conducting ring b; 7. magnetically isolating ring b; 8. magnetically conducting ring c 9. outer wall of piston head; 10. magnetic isolation ring c; 11. winding frame; 12. magnetically conducting circle d; 13. magnetically conducting ring e; 14. lower end cap of piston head

Fig. 2. (Color online) Two-dimensional schematic diagram of the valved piston head of the hybrid channel valved magnetorheological damper.

threaded to the piston rod and reinforced with thread fastening adhesive in order to prevent the piston from loosening during movement. A twining frame is arranged on the left and right sides of the piston rod winding, and the corresponding grooves are processed in the lower left and lower right respectively to match, forming a complete winding groove. Since the piston head is completely symmetrical, the fluid flow channels I and XIII are made of a clearance fit between the magnetic conducting e and the magnetic conducting disc a. In order to ensure the precise size of the fluid flow channels, four uniformly sized round table are machined on the outside of the magnetic conducting e. The lower side of the magnetic conducting ring e and the magnetic conducting ring d form the liquid flow channel II and XII. The outer side of the magnetic conducting ring a and the magnetic conducting ring d form the liquid flow channel III and XI. The two ends of the magnetic conducting disc b form the liquid flow channel IV, VI, X and VIII with the magnetic conducting ring a and the magnetic conducting ring b respectively, and the outer wall of the piston head forms the liquid flow channel V and IX, while the liquid flow channel VII is a gap fit between the magnetic conducting ring c and the two magnetic conducting rings b and the magnetic isolation ring b. In order to make the magnetic lines of force pass perpendicularly through more liquid flow channels, some non-magnetizing materials are added

Table 1. Related parameters of MRF-J25T

Project	Parameter
Density	2.65 g/cm^3
Zero field viscosity (γ = 10/s, 20 °C)	1 Pa·s
Shear stress (B = 5000 Gs)	≥45 kpa
Magnetization performance (Ms)	380 kA/m
Temperature range	-40~130 °C

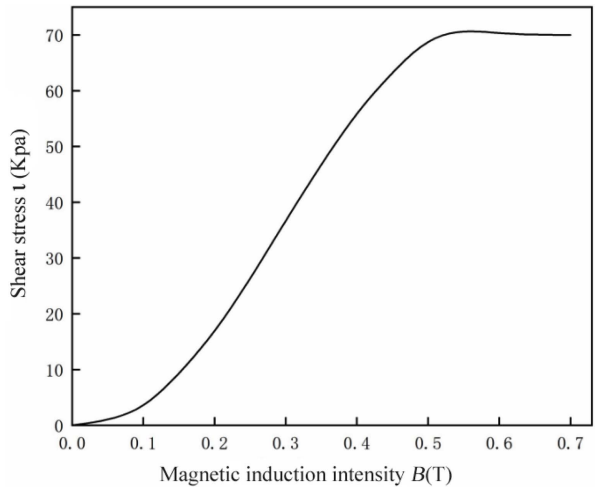

Fig. 3. τ-B relationship curve between MRF-J25T.

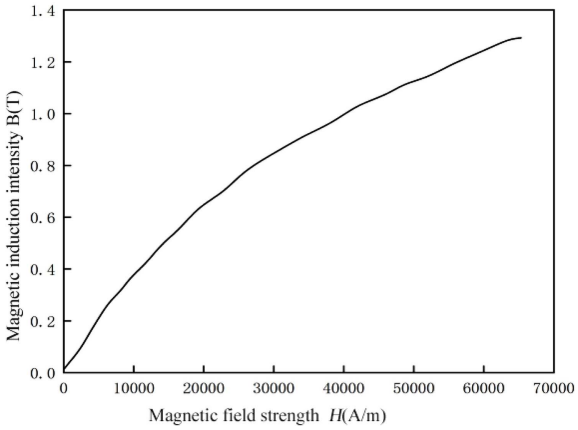

Fig. 4. B-H relationship curve between MRF-J25T.

to effectively improve the utilization of liquid flow channels.

This paper selects MRF-J25T magnetorheological fluid developed by Chongqing Instrument Materials Research Institute as the working medium of magnetorheological dampers. This type of magnetorheological fluid has good anti-deposition property, heat dissipation and stability. The correlative characteristic parameters of MRF-J25T magnetorheological fluid are shown in Table 1. The variation of shear yield strength τ with magnetic induction

strength B is shown in Fig. 3, and the magnetization curve of this type of magnetorheological fluid is shown in Fig. 4.

3. Magnetic Circuit Analysis

Figure 5 shows a schematic diagram of the magnetic circuit of the hybrid channel valve type magnetorheological damper. From the figure, can be seen that the magnetic lines start from the piston rod, due to the presence of the magnetic isolation ring a, forcing the magnetic lines to pass through the magnetic conduction ring e, liquid flow channel I, magnetic conduction disc a in turn. Due to the end cover of the magnetic isolation piston, the magnetic force line passes through the magnetic conduction disk a through the liquid flow channel II into the magnetic conduction ring d. The magnetic isolation ring c causes the magnetic field line to enter the liquid flow channel III and exit from the magnetic conductivity ring a. The outer wall of the magnetic isolation piston makes the magnetic force line parallel to the axis, passing through liquid flow channels IV, VI and magnetic conducting disk b. In order to induce the magnetic lines of force to pass through the liquid flowing channel VII, a magnetically isolating ring b is added between the two magnetic conductivity ring b so that the magnetic lines of force pass from the liquid flow channel VII through the magnetic conductivity ring c and then out from the liquid flow channel VII. Since the hybrid channel valved magnetorheological damper valved piston head is perfectly symmetrical, the other half of the magnetic lines follow the same course and converge at the piston rod to form a complete circuit. Table 2 shows the dimensional parameters of the valved piston head.

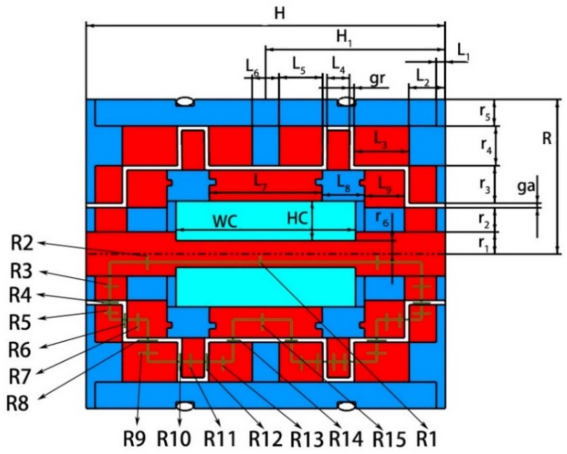

Fig. 5. (Color online) Schematic diagram of the magnetic circuit of the hybrid channel valve type magnetorheological damper.

Table 2. Dimensional parameters of valve type piston heads

Structure parameters	value (mm)
Piston head cylinder outside diameter R	30
Piston head block length H	80
Total length of coil slot WC	20
Total height of coil slot HC	9
Axial clearance gr	1
Radial clearance ga	1
Piston rod diameter r_1	5
Thickness of magnetically conductive ring e r_2	3
Thickness of magnetically conductive disc a r_3	8
Magnetically conductive ring a thickness r_4	7
Piston head block thickness r_5	6
Height of the coil slot on the piston rod r_6	3
Piston head end cap length L_2	8
Middle length of piston head end cap L_1	2
Length of the magnetically conducting ring a L_3	12
Length of magnetically conductive disc b L_4	5
Length of magnetically conductive ring b L_5	10
Length of magnetic insulation ring b L_6	6
Length of the magnetically conductive ring c L_7	26
Length of the magnetic insulation ring c L_8	9
Length of the magnetically conductive ring d L_9	9

From Fig. 5, can be seen that the magnetic lines of force pass vertically through the 8 magnetic conductors in the upper left part of the piston, while passing through 6 sections of the liquid flow channel. Since the piston head is completely symmetrical, the magnetorheological damper magnetic circuit is divided into a total of 28 effective sections. Figure 6 shows a schematic diagram of the equivalent magnetic circuit of the hybrid channel valve type magnetorheological damper.

Using Ampere's law and Ohm's law of the magnetic

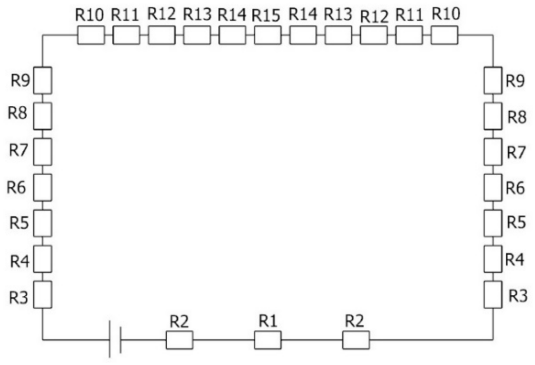

Fig. 6. Schematic diagram of the equivalent magnetic circuit of the hybrid channel valve magnetorheological damper.

circuit, we know that:

$$NI = R_m BS \tag{1}$$

Where R_m is the total reluctance of the magnetic circuit, B is the intensity of magnetic induction, S is the cross-sectional area.

In order to calculate the saturation magnetomotive force of a hybrid channel-valved magnetorheological damper, the total magnetoresistance in the magnetic circuit needs to be calculated. Assuming that magnetically conductive material is a homogeneous material, magnetoresistance can be calculated using the formula:

$$R = \frac{L}{\mu S} \tag{2}$$

Where L is the length of the magnetic line of force perpendicular to the material in the magnetic circuit, μ is the relative permeability of the material, S is the cross-sectional area of the magnetic line of force perpendicular to the magnetic materials.

1) The magnetoresistance of the piston rod is R_1, R_2

$$\begin{aligned} R_1 &= \frac{WC}{\mu_1 \pi r_6^{\,2}} \\ R_2 &= \frac{H_1 - \frac{WC}{2} - L_1}{\mu_1 \pi r_1^{\,2}} \end{aligned} \tag{3}$$

2) The reluctance of the magnetically conducting circle e is R_3

$$R_3 = \frac{r_2}{2\mu_1 \pi \left(L_2 - L_1 + gr\right)\left(\frac{r_2}{2} + r_1\right)} \tag{4}$$

3) The magnetoresistance of the permeable disc a is R_5

$$R_5 = \frac{r_3}{2\mu_1 \pi \left(L_2 - L_1\right)\left(\frac{r_3}{2} + r_1 + r_2 + ga\right)} \tag{5}$$

4) The reluctance of the magnetically conducting circle d is R_7

$$R_7 = \frac{L_9}{\mu_1 \pi \left[\left(r_1 + r_2 + r_3\right)^2 - \left(r_1 + r_2\right)^2\right]} \tag{6}$$

5) The magneto-resistance of the permeable ring a is R_9

$$R_9 = \frac{L_3}{\mu_1 \pi \left[\left(R - r_5\right)^2 - \left(R - r_5 - r_4\right)^2\right]} \tag{7}$$

6) The magnetoresistance of the permeable disc b is R_{11}

$$R_{11} = \frac{L_4}{\mu_1 \pi \left[\left(R - r_5 - ga\right)^2 - \left(R - r_5 - r_4 - ga\right)^2\right]} \tag{8}$$

7) The magnetoresistance of the magnetically conducting ring b is R_{13}

$$R_{13} = \frac{L_5}{\mu_1 \pi \left[\left(R - r_5\right)^2 - \left(R - r_5 - r_4\right)^2\right]} \tag{9}$$

8) The magnetoresistance of the magnetically conducting ring c is R_{15}

$$R_{15} = \frac{L_7}{\mu_1 \pi \left[\left(R - r_5 - r_4 - ga\right)^2 - \left(r_6 + HC\right)^2\right]} \tag{10}$$

9) The magnetoresistance of liquid flow channel I and XIII is R_4

$$R_4 = \frac{ga}{2\mu_0 \pi \left(L_2 - L_1\right)\left(r_2 + r_1 + \frac{ga}{2}\right)} \tag{11}$$

10) The magnetoresistance of fluid flow channels II and XII is R_6

$$R_6 = \frac{gr}{\mu_0 \pi \left[\left(r_1 + r_2 + ga + r_3\right)^2 - \left(r_1 + r_2\right)^2\right]} \tag{12}$$

11) The magnetoresistance of fluid flow channels III and XI is R_8

$$R_8 = \frac{gr}{2\mu_0 \pi L_9 \left(R - r_5 - r_4 - \frac{ga}{2}\right)} \tag{13}$$

12) The magnetoresistance of liquid flow channels IV, VI, X and VIII is R_{10}, R_{12}

$$R_{10} = R_{12} = \frac{gr}{\mu_0 \pi \left[\left(R - r_5\right)^2 - \left(R - r_5 - r_4 - ga\right)^2\right]} \tag{14}$$

13) The magnetoresistance of liquid flow channel VII is R_{14}

$$R_{14} = \frac{gr}{2\mu_0 \pi L_5 \left(R - r_5 - r_4 - \frac{ga}{2}\right)} \tag{15}$$

where μ_0 is the magnetic permeability of the magnetorheological fluid in the liquid flow channel: $\mu_0 = \pi \times 10^{-6} H/m$, μ_1 is the magnetic permeability of the magnetically conductive material in the damper: $\mu_1 = 4\pi \times 10^{-4} H/m$.

In summary, the total magnetoresistance of the magnetorheological dampers is

$$R_m = 2(R_1 + R_2 + R_3 + R_4 + R_5 + R_6 + R_7 + R_8 + R_9 + R_{10} + R_{11} + R_{12} + R_{13} + R_{14}) + R_{15} \quad (16)$$

By substituting the basic dimensional parameters of the valved piston in Table 1 into the above equation, it is calculated that:

$$NI = 1647 \quad (17)$$

Assuming the rated operating current required for the damper to operate is 3A, the damper needs to wind 549 turns of excitation coil to meet the requirement. The diameter of 0.6 mm enameled wire reasonably twining in the area of 360 coil slot can be wound 1000 turns, consider in the actual situation of manual twining there is a certain error, so set the twining rate of 0.7, theoretical twining line 700, in order to meet the conditions of the two, the final choice of twining 560 turns coil.

4. Mathematical Model of Damping Force

After searching for information, it is known that the damping force of the valved magnetorheological damper is mainly controlled by the pressure drop generated by the valved piston head. Therefore, in order to obtain the damping force of the hybrid channel valved magneto-rheological damper, the pressure drop generated by its fluid flow channel needs to be analyzed first. As shown in Fig. 2, the main types of fluid flow channels of this magnetorheological damper are: circular-type fluid flow channels I, III, V, VII, IX, XI, XIII; disc-type fluid flow channels II, IV, VI, VIII, X, XII. All of the above fluid flow channels generate viscous pressure drops, but not completely generate hysteresis pressure drops. The hysteresis pressure drop is due to the magnetorheological effect of the magnetorheological fluid by the magnetic field during the motion of the damper, so only the fluid flow channel through which the magnetic lines of force pass perpendicularly will generate the hysteresis pressure drop. Therefore, the liquid flow channels that produce hysteresis pressure drop are: circular liquid flow channels I, III, VII, XI, XIII; disc-type liquid flow channels II, IV, VI, VIII, X, XII. As shown in Fig. 7, the distribution of liquid flow channels is shown.

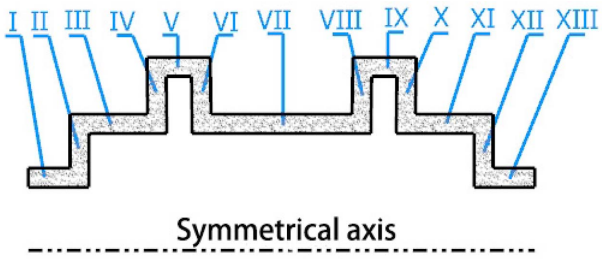

Fig. 7. (Color online) Liquid flow channel distribution diagram.

When the liquid flow channel is a ring type channel, the formula for calculating the magneto-induced pressure drop and viscous pressure drop is:

$$\triangle P_\tau = C\frac{L}{h}\tau_y(B) \quad (18)$$

$$\Delta P_\mu = \frac{6\mu L}{\pi r h^3} q \quad (19)$$

Where L is the length of the ring; h is the thickness of the ring, r is the inner radius of the ring; C is a constant, q is the flow rate of the magnetorheological fluid through the ring, μ is the viscosity of the magnetorheological fluid, ΔP_τ is the magneto-induced pressure drop, ΔP_μ is the viscous pressure drop.

The mathematical model of the pressure drop of the hybrid channel-valve magnetorheological damper is obtained by substituting the corresponding structural parameters in Table 2.

$$\triangle P_{\tau_I} = \triangle P_{\tau_{XIII}} = C\frac{L_2 - L_1}{ga}\tau_y(B) \quad (20)$$

$$\triangle P_{\tau_{III}} = \triangle P_{\tau_{XI}} = C\frac{L_9}{ga}\tau_y(B) \quad (21)$$

$$\triangle P_{\tau_{VII}} = 2\bullet C\frac{L_5}{ga}\tau_y(B) \quad (22)$$

$$\Delta P_{\mu_I} = \Delta P_{\mu_{XIII}} = \frac{6\mu L_2}{\pi\left(r_1 + r_2 + \frac{ga}{2}\right)ga^3} q \quad (23)$$

$$\Delta P_{\mu_{III}} = \Delta P_{\mu_{XI}} = \frac{6\mu(L_3 - gr)}{\pi\left(R - r_5 - r_4 - \frac{ga}{2}\right)ga^3} q \quad (24)$$

$$\Delta P_{\mu_V} = \Delta P_{\mu_{IX}} = \frac{6\mu L_5}{\pi\left(R - r_5 - \frac{ga}{2}\right)ga^3} q \quad (25)$$

$$\Delta P_{\mu_{VII}} = \frac{6\mu L_7}{\pi\left(R - r_5 - r_4 - \frac{ga}{2}\right)ga^3} q \quad (26)$$

When the liquid flow channel is a disc-shaped channel, the formula for calculating the magneto-induced pressure drop and viscous pressure drop is:

$$\Delta P_{\tau} = \frac{C(r_1 - r_2)}{r_3}\tau_y(B) \tag{27}$$

$$\Delta P_{\mu} = \frac{6\mu q}{\pi r_3^3} In\frac{r_1}{r_2} \tag{28}$$

Where r_1 is the outer diameter of the disc, r_2 is the inner diameter of the disc, r_3 is the thickness of the disc, C is a constant, q is the flow rate of the magnetorheological fluid through the ring, μ is the viscosity of the magnetorheological fluid, ΔP_{τ} is the magneto-induced pressure drop, ΔP_{μ} is the viscous pressure drop.

Substitute the structural parameters in Table 1 to obtain the mathematical model of the pressure drop of the hybrid channel-valved magnetorheological damper as:

$$\Delta P_{\tau_{II}} = \Delta P_{\tau_{XII}} = \frac{C\left[(R - r_5 - r_4) - (r_1 + r_2)\right]}{gr}\tau_y(B) \tag{29}$$

$$\begin{aligned}\Delta P_{\tau_{IV}} &= \Delta P_{\tau_{VI}} = \Delta P_{\tau_{VII}} = \Delta P_{\tau_X} \\ &= \frac{C\left[(R - r_5) - (R - r_5 - r_4 - ga)\right]}{gr}\tau_y(B)\end{aligned} \tag{30}$$

$$\Delta P_{\mu_{II}} = \Delta P_{\mu_{XII}} = \frac{6\mu q}{\pi gr^3} In\frac{R - r_5 - r_4}{r_1 + r_2} \tag{31}$$

$$\begin{aligned}\Delta P_{\mu_{IV}} &= \Delta P_{\mu_{VI}} = \Delta P_{\mu_{VII}} = \Delta P_{\mu_X} \\ &= \frac{6\mu q}{\pi gr^3} In\frac{R - r_5}{R - r_5 - r_4 - ga}\end{aligned} \tag{32}$$

The total pressure drop of the hybrid channel valved magnetorheological damper is the sum of the magneto-induced pressure drop and viscous pressure drop generated by the fluid flow channel, so the total pressure drop ΔP is:

$$\begin{aligned}\Delta P &= \Delta P_{\mu} + \Delta P_{\tau} \\ &= \Delta P_{\mu_I} + \Delta P_{\mu_{XIII}} + \Delta P_{\mu_{III}} + \Delta P_{\mu_{XII}} + \Delta P_{\mu_V} + \Delta P_{\mu_{IX}} \\ &+ \Delta P_{\mu_{VII}} + \Delta P_{\mu_{II}} + \Delta P_{\mu_{XII}} + \Delta P_{\mu_{IV}} + \Delta P_{\mu_{VI}} + \Delta P_{\mu_{VII}} + \Delta P_{\mu_X} \\ &+ \Delta P_{\tau_I} + \Delta P_{\tau_{XIII}} + \Delta P_{\tau_{III}} + \Delta P_{\tau_{XI}} + \Delta P_{\tau_{VII}} + \Delta P_{\tau_{II}} + \Delta P_{\tau_{XII}} \\ &+ \Delta P_{\tau_{IV}} + \Delta P_{\tau_{VI}} + \Delta P_{\tau_{VII}} + \Delta P_{\tau_X}\end{aligned} \tag{33}$$

From Pascal's law, the output damping force of the hybrid channel valve magnetorheological damper F is:

$$F = \Delta P \bullet S \tag{34}$$

Where: S is the contact area between the piston head of the hybrid channel valve type magnetorheological damper and the magnetorheological fluid.

Adjustable range of damping force output:

$$K = \frac{F}{F_{\mu}} = \frac{F}{\Delta P_{\mu} \bullet S} \tag{35}$$

5. Results Analysis and Discussion

5.1. Simulation process

In order to verify the good damping performance of the hybrid channel-valve magnetorheological damper, ANSYS is used to simulate it in the electromagnetic field. For ease of calculation, a simplified model is built using 1/2 of it. As shown in Fig. 8(a), the two-dimensional simulation model of the hybrid channel-valved magnetorheological damper; (b) the device material is given; (c) the magnetic force line distribution diagram. From figure (b), can be seen that the red area indicates the non-magnetizing materials, the purple part is the coil, the cyan is the magnetizing material, and the blue part is the liquid flow channel. From the figure (c), can be seen that the magnetic lines of force pass almost perpendicularly through all the magnetic flow channels.

5.2. Effect of current size on damping force

From the magnetic circuit design, it is clear that when the basic structure of the damper is determined, the only

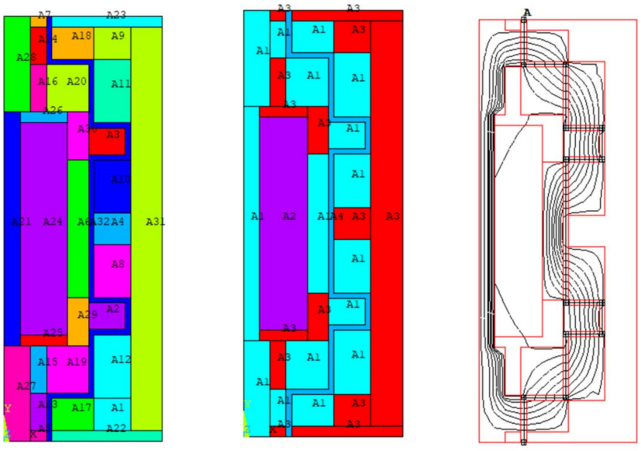

(a) (b) (c)

Fig. 8. (Color online) Two-dimensional simulation model of hybrid channel-valved magnetorheological damper. (a) Two-dimensional model, (b) Device material endowment diagram, (c) Magnetic force line distribution diagram.

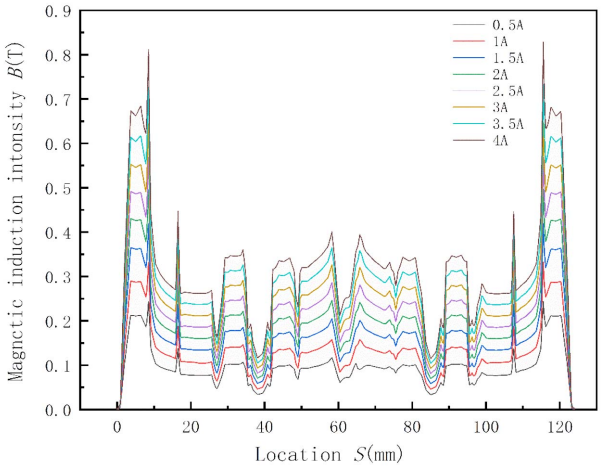

Fig. 9. (Color online) Variation of magnetic induction intensity in the damping gap for different current magnitudes.

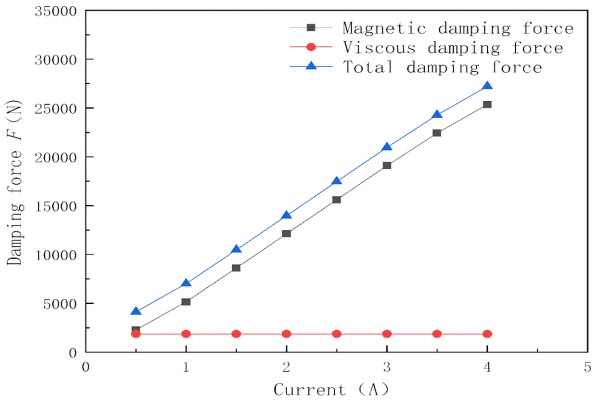

Fig. 10. (Color online) Effect on output damping force at different current levels.

factor that affects the magnetic induction strength is the current. Since the magnetic induction strength of magnetorheological fluid used saturates at 0.5 T, it is crucial to study the effect of current on the damping performance in order to reduce energy waste. Figure 9 shows the variation of magnetic induction intensity in the damping gap at different current magnitudes for a coil turn number of 560, an axial gap of 1 mm, and a radial gap of 1 mm. It is obvious from the graph that the magnetic induction strength of the damping gap increases with the increase of current, which is due to the increase of current and the enhancement of the generated magnetic field strength.

Figure 10 shows the effect of different current magnitudes on the output damping force of magnetorheological dampers. As shown in equation (18-32), the magnetic damping force is related to the current magnitude, and the viscous damping force is not related to the current

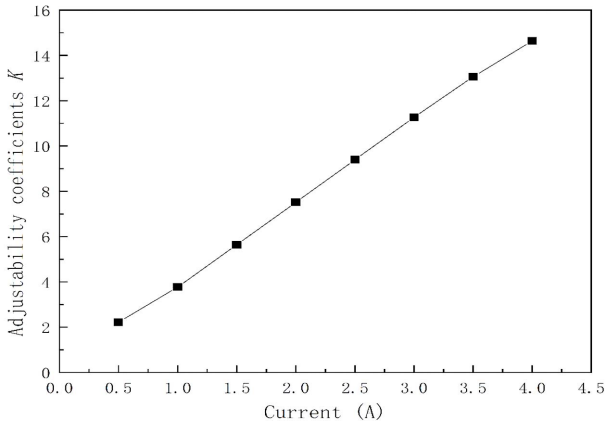

Fig. 11. Effect on the adjustable coefficient for different current levels.

magnitude. It is obvious from the figure that the size of the hysteresis damping force increases with the increase of the current, which is because the size of the current will make the magnetic induction strength B enhanced, thus making the enhancement of τ. From the magnetic damping force formula, it is known that the magnetic damping force F is proportional to τ. Therefore, the total damping force of the damper will increase with the increase of the magnetic damping force in the case of constant viscous damping force. Figure 11 shows the effect on the adjustable coefficient for different current magnitudes. From the formula of adjustable coefficient, it can be seen that the adjustable coefficient increases with the increase of magnetic damping force under the condition of constant viscous damping force.

5.3. Effect of axial clearance on damping performance

From the damping force equation, can be seen that the output damping force of magnetorheological dampers is closely related to the axial clearance of the damping channel. In order to obtain magnetorheological dampers with good performance, it is necessary to investigate the non-effects caused by different axial clearances. The effect of different axial clearances on the magnetic induction intensity is shown in Fig. 12. As can be seen from the figure, with the increase of the axial damping gap, the magnetic induction strength at the axial gap obviously shows a decreasing trend, which is because with the increase of the axial gap, the magnetic resistance at the axial gap will show a rising trend, and when the total magnetic flux is certain, the magnetic induction strength will be reduced.

By numerical calculation, the variation of damping performance of the hybrid channel-valved magnetorheological dampers at different axial clearances can be known.

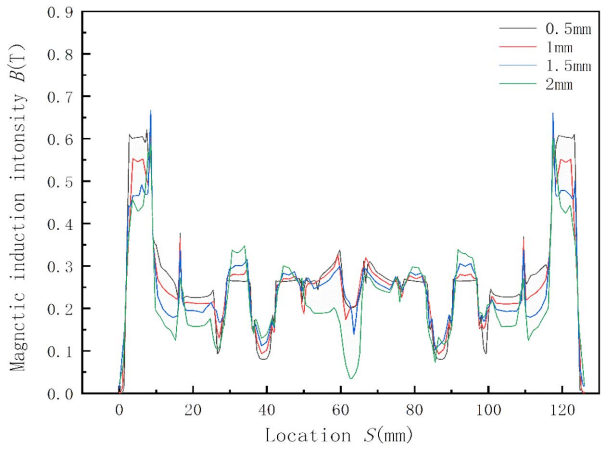

Fig. 12. (Color online) Effect of different axial clearances on magnetic induction intensity.

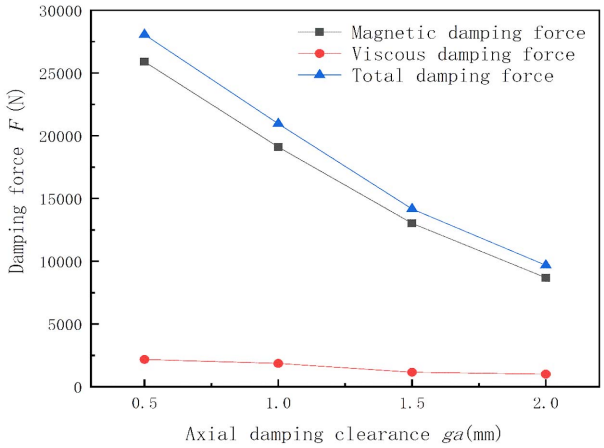

Fig. 13. (Color online) Effect of different axial clearances on the output damping force of magnetorheological dampers.

Figure 13 shows the effect of different axial clearances on the output damping force of the magnetorheological damper, and it is obvious that the damping force decreases as the axial clearance increases, because the damping force is inversely proportional to the axial clearance in the mathematical model of the damper. Figure 14 shows the influence of different axial clearances on the adjustable coefficient of the Mr Damper. As can be seen from the figure, when the axial clearance is 0.5-1 mm and 1.5 mm-2 mm, the adjustable coefficient tends to decrease. When 1 mm-1.5 mm, the adjustable coefficient increases gradually. This is because the adjustable coefficient is controlled by both viscous and magnetic damping forces. When the adjustable coefficient rises, the rising rate of the magnetic damping force is faster than that of the viscous damping force. When the adjustable coefficient decreases, the decreasing rate of the magnetic damping force is faster than that of the viscous damping force.

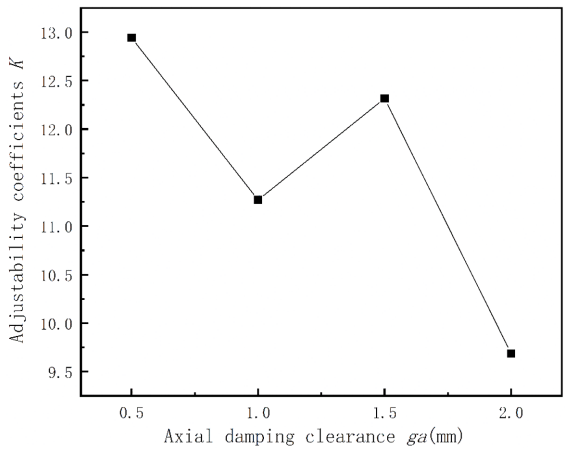

Fig. 14. Influence on the adjustable coefficient with different axial clearances.

5.4. Effect of radial clearance on damping performance

Since this paper studies the mixed fluid flow channel, the effect of radial clearance on the damping performance also needs to be studied. As shown in Fig. 15, the effect of different radial gaps on the magnetic induction strength, can be seen that as the radial damping gap increases, the magnetic induction strength at the radial gap is obviously decreasing, the reason is the same as that of the axial gap.

Similarly, by numerical calculation, the damping performance of the hybrid channel-valved magnetorheological dampers with different radial directional clearances can be known. Figure 16 shows the effect of different radial gaps on the output damping force of the magnetorheological

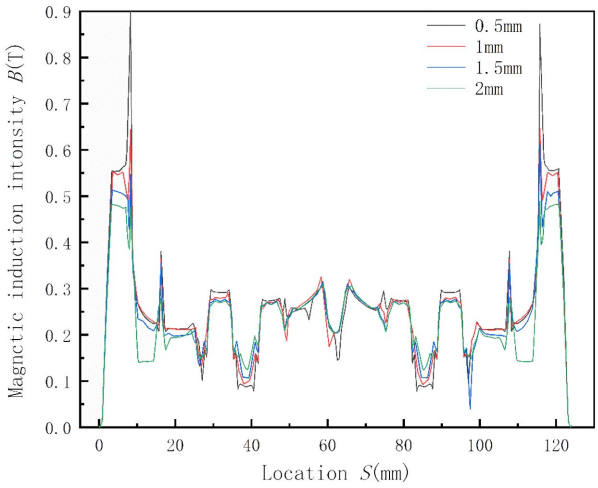

Fig. 15. (Color online) Effect of different radially oriented gaps on the magnetic induction intensity.

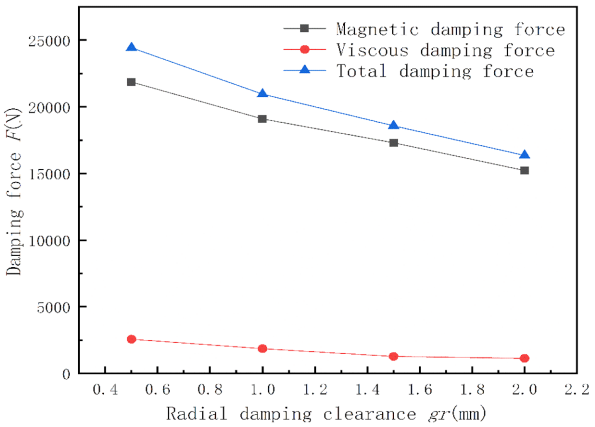

Fig. 16. (Color online) Effect on damping force with different radial clearance.

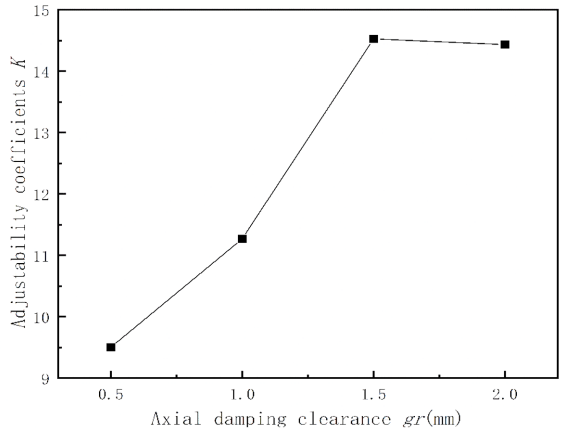

Fig. 17. Influence on the adjustable coefficient with different radial clearances.

damper, and it is obvious that the damping force decreases as the radial gap increases, because the damping force is inversely proportional to the radial gap in the mathematical model of the damper.

Figure 17 shows the effect of different radial clearances on the adjustable coefficient of the magnetorheological damper and it can be seen from the graph that the adjustable coefficient tends to rise when the axial clearance is 0.5-1.5 mm. The adjustable coefficient tends to decrease slowly at 1.5 mm-2 mm. This is because when the axial gap is 0.5-1.5 mm. The magnetic damping force rises faster than the viscous damping force. At 1.5-2 mm. The decrease rate of magnetic damping force is faster than that of viscous damping force.

6. Conclusion

(1) In this paper, a hybrid channel valved magneto-rheological damper is designed, which has five circular channels and four disc channels interleaved in series. In order to compensate for the low utilization rate of the liquid flow channel on both sides of the coil and the upper part of the coil, the arrangement of the magnetic separation material is used to influence the direction of the magnetic lines, so that more magnetic lines can pass through the liquid flow channel and effectively improve the utilization rate of the magnetic field.

(2) The output damping force of the mixed-channel valved magnetorheological damper increases with the increase of current under the influence of current; It decreases with the increase of clearance under the change of axial clearance and radial clearance.

(3) From the simulation results, it can be seen that the output damping force F of the hybrid channel valved magnetorheological damper is 18 KN and the adjustable coefficient K is 14.52 with the current I of 3A, the number of coil turns of 560, the axial gap ga of 1mm and the radial gap gr of 1.5 mm.

References

[1] J. Rabinow, IEEE (1948).
[2] K. Q. Yang and H. Huang, Journal of Shenyang University of Technology **41**, 1 (2022).
[3] J. P. Du, Harbin Institute of Technology (2021).
[4] X. J. Guo, J. Zhao, X. C. Zhang, and J. Jing, Building Structure **51**, 12 (2021).
[5] Z. Jian, X. H. Liu, Z. J. Ding, and Z. N. Zhi, Machine Tools and Hydraulics **49**, 23 (2021).
[6] F. Zhang, Ship Science and Technology **44**, 4 (2022).
[7] C. Qi, B. Xu, J. Yu, and S. Yang, Journal of Automotive Safety and Energy Conservation **13**, 2 (2022).
[8] H. N. Qi, G. L. Hu, and L. F. Yu, Mechanical Design **39**, 2 (2022).
[9] S. S. Zhu, L. B. Tang, J. G. Liu, X. Z. Tang, X. W, Shock and Vibration, 8086504 (2016).
[10] H. Yi, L. L. Dong, and C. F. Hao, International Journal of Applied Electromagnetics and Mechanics **59**, 1 (2019).
[11] G. L. H, H. Liu, J. F. Duan, and L. F. Yu, Advances in Mechanical Engineering **11**, 1 (2019).
[12] S. Doruk and H. Gurocak, Mechatronics **20**, 3 (2010).
[13] K. Kim, Z. Chen, D. Yu, and C. Rim, Smart Materials and Structures **25**, 7 (2016).
[14] R. Zemp, J. C. D. L. Llera, H. Saldias, and F. Weber, Smart Materials and Structures **25**, 10 (2016).
[15] I. I. M. Yazid, S. A. Mazlan, T. Kikuchi, H. Zamzuri, and F. Imaduddin, Materials and Design 54 (2014).